Organelle resolved proteomics reveals new chordoma cell surface markers required for proliferation and association with outcome

Shahbaz Khan
University Health Network
Jeffrey Zuccato
University of Toronto
Vladimir Ignatchenko
University Health Network
Olivia Singh
University Health Network
Meinusha Govindarajan
University Health Network
Matthew Waas
University Health Network
Andrew Gao
University Health Network
Gelareh Zadeh
University of Toronto
Thomas Kislinger (thomas.kislinger@utoronto.ca)
University Health Network

Research Article

Keywords: Organelle fractionation, proteomics, cell surface proteins, chordoma

Posted Date: April 13th, 2022

DOI: https://doi.org/10.21203/rs.3.rs-1534853/v1

Abstract

Background

Chordomas are rare, clinically aggressive tumors with a median survival of 6-7 years and a high rate of disease progression despite maximal surgery and radiotherapy. Given the limited options available to prevent and treat progression and relatively poor prognosis, there remains an urgent need for the development of novel therapies to improve clinical outcomes. Cell-surface proteins are attractive therapeutic targets due to their accessible subcellular localization.

Methods

Here, we used a proteomics approach to identify novel chordoma-specific cell-surface protein markers. Four established chordoma cell lines were analyzed by quantitative proteomics using a comprehensive differential ultracentrifugation organellar fractionation approach. A subtractive proteomics strategy was applied to select proteins that are plasma membrane enriched. Using commercially available antibodies, the expression profiles of these cell-surface proteins were validated across chordoma cell lines, patient surgical tissue samples, and normal tissue lysates via Western blotting. The candidates were further validated by immunohistochemical analysis in a 25-patient tissue cohort. Finally, the essentiality of these candidates for *in vitro* chordoma growth was evaluated.

Results

Mass spectrometry-based proteomics identified 120 high-confidence cell-surface proteins in four established chordoma cell line models. Systematic data integration prioritized two chordoma-specific cell surface proteins for further interrogation. Immunohistochemistry in a richly annotated cohort of chordoma tumor tissues revealed that PLA2R1 and SLC6A12 are broadly expressed in chordoma patient samples. Higher expression of PLA2R1 correlated with poor prognosis whereas SLC6A12 expression was significantly enriched in skull-base chordomas compared to those arising in the spine. Using a siRNA-mediated knockdown of PLA2R1, we demonstrated significant inhibition of cell growth and colony-forming ability, suggesting these proteins play an essential role in chordoma biology.

Conclusion

We have comprehensively elucidated the proteome of four established chordoma cell lines. Subtractive proteomics and integrative data mining revealed novel cell-surface proteins required for chordoma cell survival and associated with clinical parameters in a small chordoma tissue sample cohort.

Background

Chordoma is a rare but devastating bone cancer of the skull base and spine with an incidence of 8 cases per ten million people per year (1). Chordoma patients experience a relatively high mortality compared to more benign tumor types, with a 10-year survival rate of 40%. Patients also experience morbidities

associated with chordoma progression during the course of their disease as 30–85% experience tumor recurrence and invasion into surrounding neurological structures as well as one-third of cases metastasize to other organs (2). There is growing interest in identifying new targeted therapy options to treat chordomas both upfront after surgery/radiotherapy, and after later tumor recurrence, in order to improve these outcomes. Such novel targeted therapies may be preferentially considered for patients who underwent a subtotal surgical resection or have poorly prognostic molecular signatures, thereby leading to further personalized clinical care (3). Previous studies using whole genome (WGS) (4), whole exome (WES) (4, 5), and RNA sequencing (4–6) have shown a high degree of genetic heterogeneity between chordoma tumors and no robust targetable biomarkers have been identified to date. Targeted therapies for chordoma patients are hence limited to early clinical trials (4, 5). Accordingly, novel approaches to identifying new therapeutic targets are needed and could be transformative for patient care.

Aberrations from homeostatic protein expression, either through somatic mutations or large-scale genomic amplifications/deletions, lead to rewiring of essential signalling pathways that drive cancer initiation and progression (7). Importantly, these changes are difficult to predict from genomic and transcriptomic data and require direct quantitation at the proteome level, which has not been comprehensively performed in chordoma to date. Mass spectrometry-based proteomic approaches can inform spatial localization of proteins which other omic technologies cannot provide (8). Cell-surface proteins carry out essential cellular functions such as cell-cell interactions, ion transport and cell signalling transduction pathways (9). Surface proteins are attractive drug targets as they are readily accessible through small molecules, therapeutic antibodies, or other immunotherapies (9, 10). In this study we used a proteomics-based approach to identify novel cell-surface proteins in chordoma cell lines. Following integrative data mining, we discovered two chordoma-enriched cell surface proteins for further investigation. These include Secretory phospholipase A2 receptor (PLA2R1) and Sodium- and chloride-dependent betaine transporter (SLC6A12), also known as Betaine-GABA transporter (BGT1). We investigated the expression of these cell surface proteins in a richly annotated cohort of patient tumors and assessed their correlation to clinical factors as potential biomarkers. Furthermore, siRNA-mediated knockdown studies were conducted to explore the requirement of these proteins for chordoma cell growth and survival and highlight relevance as candidates for future therapeutic intervention.

Methods

Cell Culture

The chordoma cell lines U-CH17P, U-CH17M, U-CH17S, U-CH11R, UM-Chor1 and MUG-chor1 were generously provided by the Chordoma Foundation (www.chordomafoundation.org). The cells were grown IMDM/RPMI 1640 (4:1; Sarstedt Inc) supplemented with 10% FBS and penicillin-streptomycin-glutamine (PSG; 100 U/mL penicillin, 100 µg/mL streptomycin, 292 µg/mL L-glutamine) (Gibco, Ontario, Canada). The cells were maintained in a humidified 37°C incubator with 5% CO_2 until confluency.

Silica-bead based cell surface protein capture

Cell surface protein capture was performed as previous described (11, 12) with minor modifications. The chordoma cell lines (U-CH17P, U-CH17M, U-CH17S and U-CH11R) were washed three times with ice-cold MBS buffer (25 mM MES, 150 mM NaCl pH 6.5) and a monolayer of cells were overlaid with 20 mL of 1% colloidal silica bead (LUDOX® CL colloidal silica suspension in water) with gentle shaking for 15 minutes at 4°C. Excessive beads were removed, and the plates were washed three times with MBS buffer. 20 mL of 0.1% Polyacrylic acid (PAA)in MBS buffer was added to the cells with gentle shaking for 15 minutes at 4°C. PAA was removed from the plates and fresh sucrose/HEPES buffer (250 mM sucrose, 25 mM HEPES pH 7.4 and 20 mM KCL) was added. Cells were scraped from the plate and centrifuged at 300 xg for 5 minutes. The supernatant was discarded, and the pellet was added to fresh sucrose/HEPES buffer. Cells were lysed by 3 cycles of sonication (35% amplitude, 10 seconds). A discontinuous Histodenz density gradient in sucrose/HEPES was prepared at different concentrations (45%,50%,55% and 60%) and layered in a 13.2 mL (Beckman) ultracentrifugation tube. The samples were diluted with Histodenz to a final concentration of 20% and added on top of the Histodenz gradient. The samples were centrifuged at 100,000 xg for 2 hours in a SW 41Ti rotor (Beckman). After the centrifugation, the density gradient layers were removed, and the resulting pellet was washed with sodium carbonate (pH 12) solution via rotation for 15 minutes at 4°C. The beads were centrifuged at 5,000 xg for 20 minutes in a benchtop centrifuge and the supernatant was removed. Elution buffer (400mM NaCl, 25mM HEPES, 1% Triton X- 100, pH 7.4) was added to the beads and rotated overnight at 4°C to elute membrane proteins from the silica beads. The eluted proteins were precipitated with ice cold acetone overnight at -20°C. The samples were pelleted at 10,000 xg for 10 mins and the resulting pellet was solubilized with 100 µL of lysis buffer (50% (v/v) 2,2,2,-Trifluoroethanol (TFE) and 50% PBS).

Subcellular fractionation and protein extraction

Subcellular fractionations were performed as previously described (13, 14) with minor modifications. Chordoma cell lines (U-CH17P, U-CH17M, U-CH17S and U-CH11R) were pelleted and washed three times with PBS. Cells were homogenised in lysis buffer (50 mM Tris-HCL (pH 7.4), 5mM $MgCl_2$, 0.1% Triton X-100 and Protease inhibitors) and kept on ice for 10 mins, and further homogenised with a loose-fitting pestle. Sucrose was added to the lysates to a final concentration of 250 mM (isotonic solution). All the subsequent steps were done at 4°C. The lysates were centrifuged at 800 xg for 15 minutes in a benchtop centrifuge (Eppendorf 5430R) at 4°C to separate the nuclear fraction. The resulting supernatant served as the source of cytosol, mitochondria and microsomes (i.e., mixed membranes). The nuclear pellet was further resuspended in 2.5 mL of cushion buffer (2M sucrose, 50 mM Tris-HCl, 5 mM $MgCl_2$, 1 mM dithiothreitol (DTT) and Protease inhibitors – Roche) and overlaid on 2 mL of cushion buffer in ultra-clear open top 5 mL ultracentrifugation tube (Beckman) and centrifuged at 80,000 xg for 45 minutes (Beckman SW 55Ti rotor). The mitochondrial fraction was isolated from the crude lysate by centrifugation at 8000 xg for 15 minutes. The resulting pellet was washed with a lysis buffer and spun again to retrieve the mitochondrial fraction. The resulting supernatant was centrifuged at 150,000 xg for 1 hour (Beckman SW 55Ti) to isolate the microsomal pellet (mixed membranes). The supernatant served as the cytosolic fraction. Nuclear proteins were extracted from the nuclear fraction with a lysis buffer (20 mM HEPES, 400 mM NaCl, 0.2mM EDTA) and rotated for 30 mins at 4 degrees. The pellet was passed through 18-guage

needle several times and centrifuged at 9000 xg for 10 mins to isolate the soluble nuclear fraction and insoluble pellet. The resulting organelle pellets (mitochondria, nuclear and microsome) were lysed in 100 µL of lysis buffer (50% (v/v) 2,2,2,-Trifluoroethanol (TFE) and 50% PBS).

Sample preparation for shotgun proteomics

The pellets obtained from the subcellular fractions were lysed by repeated freeze-thaw cycles (5 cycles, switching between a dry ice/ethanol bath and 60°C water bath) in lysis buffer. Samples were sonicated on a ultrasonic block sonicator for five 10s cycles at 10 watts per tube (Hielscher VialTweeter) followed by extraction at 60°C for 1 hour. Disulphide bonds were reduced with 5mM DTT, followed by 30 min incubation at 60°C. Free sulfhydryl groups were alkylated by incubating the samples with 25 mM iodoacetamide in the dark for 30 minutes at room temperature. The samples were diluted (1:5) with 100 mM ammonium bicarbonate (pH 8.0) and 2 mM $CaCl_2$ was added. Proteins were digested overnight with 2 µg of trypsin/Lys-C enzyme mix (Promega) at 37°C. Peptides were desalted by C18-based solid phase extraction, then dried in a SpeedVac vacuum concentrator. Peptides were solubilized in mass spectrometry-grade water with 0.1% formic acid. Liquid chromatography was directly coupled to an Orbitrap Fusion Tribrid (Thermo Scientific) and data was acquired as previously described (15, 16). Raw files were searched using the MaxQuant software (version 1.5.8.3) against a Uniprot human sequence database (number of sequences 42,041) with an FDR set to 1% for positive peptide spectral matches and protein identification using a target-decoy strategy (14). Searches were performed with maximum of two missed cleavages, oxidation of methionine residues as a variable modification, and carbamidomethylation of cysteine residues as a fixed modification. Intensity-based absolute quantification (iBAQ) and label-free quantitation (LFQ) were enabled, with match between runs function disabled due to the differences in organellar proteomes. Subsequent analyses were performed using the proteinGroups.txt file. Contaminant sequences and matching decoy were removed, and proteins identified with two or more unique peptides were carried forward. iBAQ intensities were used for protein quantitation. The data was median normalised and missing values were imputed with low values (between 1 and 1.2 $\log_2$ values).

Western blot

Chordoma cell line pellets and frozen chordoma tissue samples were lysed in RIPA buffer (50 mmol/L Tris pH 7.5, 150 mmol/L NaCl, 2 mmol/L EDTA pH 8.0, 0.5% (v/v) Triton X-100, and Complete protease inhibitor cocktail - Roche, Switzerland). The cells were kept on ice for complete lysis. Cell debris was removed by centrifugation at 16,000 xg for 10 mins at 4°C. The protein concentration was determined by BCA assay (Thermo scientific). Commercially available normal tissue lysates from various organs (Brain cortex, cerebellum, skin, stomach, esophagus and spleen) were purchased from Takarabio (USA). Gels were loaded with 10 µg of protein lysates per lane and proteins were separated on 7, 8 or 13% SDS-PAGE gels. The resolved proteins were wet transferred to polyvinylidene fluoride membrane (PVDF) and membranes were incubated in 5% (w/v) milk in Tris-buffered saline Tween-20 (TBST; 10 mmol/L Tris-Base, 150 mmol/L NaCl, 0.05% Tween-20; pH 7.4) for 1 hour. After blocking, membranes were incubated with primary antibodies (1:1000 mouse anti-human monoclonal PLA2R1, [Sigma], 1:1000 mouse anti-

human polyclonal SLC6A12 [ThermoFisher Scientific], 1:1000 rabbit anti-human monoclonal Brachyury [Cell Signaling], 1:1000 mouse anti-human monoclonal Lamin B1 [abcam] and 1:1000 rabbit anti-human monoclonal ß-actin [Novus biologicals]) overnight at 4°C.

Immunohistochemical analysis

A cohort of 25 chordoma patients with formalin-fixed paraffin (FFPE) embedded slides and clinical follow up data were obtained from the University Health Network Brain Tumor Biobank (REB# – 18-5820). Slides with 5 µm FFPE tissue sections were rehydrated with serial dilutions of ethanol followed by water and pH 6 sodium citrate dihydrate buffer was used for heat-mediated antigen retrieval. A 3% hydrogen peroxide in methanol solution was utilized to block endogenous peroxidase activity. Blocking solution (5% bovine serum albumin in phosphate buffered saline plus 0.1% Triton X-100) was applied to slides for 1 hour at room temperature. Subsequently, primary antibodies including anti-SLC6A12 (Invitrogen, PA5-57099, rabbit polyclonal antibody) and anti-PLA2R (Millipore Sigma, MABC942, mouse monoclonal antibody) were applied overnight at 4˚C diluted (1:200, 1:200, 1:250, respectively) in blocking solution. A 1 hour incubation with secondary antibody was performed followed by processing with the DAKO polymer-HRP system and DAB peroxidase kit, counterstaining with hematoxylin, tissue dehydration, and slide cover slipping. Whole slide digital scanning was performed on all slides and images were analyzed using the HALO Image Analysis Platform (Indica Labs). Each slide was annotated with multiple regions of interest to delineate chordoma tumor tissue. Three independent reviewers assessed slides for all cases (JAZ, OS, and an experienced neuropathologist AG) and representative images were selected. Proportions of stain positive cells were quantified using the HALO software algorithm, defined to identify cells with either membranous or cytoplasmic staining as a fraction of all cells. This algorithm was applied to all annotated tissue sections in an unbiased systematic manner. Wilcoxon's rank sum test was used to compare values between skull base and spinal chordomas. Univariable and multivariable Cox models were utilized to assess the prognostic utility of stain proportions together with known major prognostic clinical factors (extent of surgical resection and radiotherapy use). For survival analyses results, the upper tertile of PLAR2 values (samples with higher marker positivity) were compared to the lower two tertiles of values.

siRNA knockdown and Clonogenic assay

The chordoma cell lines (U-CH17M, U-CH17S and UM-chor1) were seeded in 6-well plates at a density of 2,000 cells per well in DMEM/RPMI media and transfected with three siRNA for PLA2R1 (Cat# SR307882, Origene), SLC6A12 (Cat# SR304423, Origene) and scrambled siRNA (negative control) (Cat# SR30004, Origene) at a concentration of 5 nM using lipofectamine RNAiMax transfection reagent (Invitrogen). After 2 weeks colonies were stained with crystal violet staining (0.5% crystal violet, 25% methanol) and the quantification of the colonies was performed using ImageJ (version).

Statistical analysis

All the proteomics experiments were performed in triplicates. Applicable data were analyzed and represented using the R statistical environment (v3.6.3). Differential expression analysis was performed

using unpaired Welch's t-test for statistical analysis, and Benjamini & Hochberg adjusted p-value < 0.05 deemed as statistically significant. Visualization in R was performed using the ggplot2 (3.2.1) and Complexheatmap (v2.2.2).

Results

Subcellular fractionation and plasma membrane enrichment

To explore the surface proteome of chordoma cell lines (Fig. 1A), we utilized a subtractive proteomics approach (17) that combined silica bead-based plasma membrane capture with organelle fractionation using differential ultracentrifugation (Fig. 1B). Organelle fractionation resulted in the enrichment of five subcellular components (plasma membrane, cytosol, mitochondria, membrane derived microsome and two nuclear fractions). In total, 72 liquid chromatography mass spectrometry (LC-MS) runs were performed, resulting in the detection of 7688 proteins (**Figure S1A; Table S1**). Principal component analysis (PCA) of the fractions revealed high degrees of similarity between different organelle proteomes regardless of cell line status, indicating that the subcellular and surface fractionation methods produce distinct mass spectrometry profiles that correspond to each isolated organelle (**Figure S1B**). Furthermore, unsupervised hierarchical clustering revealed four distinct proteomic clusters separated based on each organelle that coincided with subcellular localization annotations from publicly available databases (Fig. 2). The cluster 1 showed nuclear protein enrichment (**Figure S1C**), while cluster 2 and 3 indicated cytosolic and mixed membrane protein enrichment (**Figure S1D-E**), respectively. Cluster 4 was enriched in proteins with known or predicted cell-surface localization (**Figure S1F**).

An integrative data mining strategy was applied to identify high-confidence cell surface proteins for functional evaluations. First, a subtractive proteomics approach that compared protein expression in the silica-bead fraction (plasma membrane) against all other organelles to detect differentially abundant proteins (FDR < 0.05, $|\log_2 FC| > 1$, Mann-Whitney U-test) separately in each cell line **(Figure S2A)**. To further increase our confidence in the surface localization of our candidates, we leveraged surface prediction annotations through the use of a cell-surface protein bioinformatics tool termed SurfaceGenie (18) (https://www.cellsurfer.net/surfacegenie), in which Genie score (GS) of ≥ 20 and Surface prediction consensus score (SPC) of ≥ 3 was used as cut-off value (**Table S1**). Finally, we required surface proteins to be upregulated in plasma membrane fraction in 2 or more chordoma cell lines **(Figure S2B)**. Applying these criteria resulted in prioritization of 120 highly enriched cell surface proteins (Fig. 3A).

To identify novel targets with chordoma specific expression, we next proceeded to evaluate these 120 high confidence cell surface proteins using public proteomics data of 142 cancer cell lines (19–22). This resulted in 23 cell surface proteins with limited expression in these data (≤ 5 cancer cell lines) (Fig. 3B). As we were interested in individually interrogating select targets, we did not further consider proteins that had poor antibody availability as determined by lack of immunohistochemistry (IHC) data or an antibody reliability annotation of “Uncertain” in Human Protein Atlas (HPA). We next assessed the normal tissue expression of the remaining 15 chordoma specific cell-surface proteins using publicly available normal

tissue datasets (Fig. 3B). Specifically, we ranked the set of proteins by the proportion of normal tissue in which they were not detected by IHC in HPA (version 20.1) (23), median protein expression in two normal tissue MS-based proteomics datasets (24, 25), and median RNA expression in the GTEx normal tissue RNA-seq database (26). Proteins were prioritized based on the rank sum of the four individual normal tissue rankings (Fig. 3C). The top two cell-surface proteins, Secretory phospholipase A2 receptor (PLA2R1) and Sodium- and chloride-dependent betaine transporter (SLC6A12) (Fig. 3C; **Figure S3A-H)** were selected for further interrogation.

Validation of chordoma surface markers

After shortlisting two highly enriched surface proteins, commercial antibodies were utilized to evaluate their expression by Western blotting in the chordoma cell lines. After evaluation of these antibodies in chordoma cell lines, additional chordoma tissue lysates and commercially available normal tissue lysates were tested for the expression of these target proteins through Western blotting. As Brachyury is a diagnostic biomarker of chordoma, its expression was also confirmed in the chordoma cell lines and chordoma tissue samples. We were able to validate higher expression of PLA2R1 and SLC6A12 in the chordoma cell lines and the chordoma tumor tissue samples, compared to normal tissues lysates (Fig. 4A). An additional two chordoma cell lines (UM-Chor1 and MUG-Chor1) were also used to confirm expression of these two targets **(Figure S4A).** Consequently, evaluation of tissue expression by immunohistochemistry and functional analysis were performed.

Immunohistochemistry indicates clinicopathologic significance of cell-surface proteins

Surgical chordoma tissue samples were evaluated by IHC using available antibodies against PLA2R1 and SLC6A12 to validate our *in vitro* chordoma data and assess their utility as clinical biomarkers. PLA2R1 and SLC6A12 expression was observed in patient chordoma tumor samples and localized mainly to cell membranes. (Fig. 4B,D). SLC6A12 positive cells were identified in a majority of samples with median (interquartile range) cellularity values being 38.6% (21.1–57.9%), respectively. Additionally, the proportion of SLC6A12 positive cells was higher in skull base than spinal chordomas (Fig. 4B,C: **47.8 vs. 21.9%, p = 0.032**). Table 1 shows the prognostic utility of PLA2R1 staining proportion, where samples with higher tertile cellularity values experienced a worse progression-free interval (PFI: HR = 5.2, 95% CI = 1.5–17.5, p = 0.0078) and overall survival (OS: HR = 6.7, 95% CI = 1.7–27.0, p = 0.0076) in univariable Cox analyses. When combined with extent of resection and adjuvant radiotherapy receipt as known prognostic factors in multivariable Cox analyses, PLA2R1 staining extent was independently prognostic with statistical significance for both PFI (HR = 7.8, 95% CI = 1.8–32.7, p = 0.0052) and OS (HR = 11.5, 95% CI = 1.6–80.7, p = 0.0144). Representative tumor tissue images of differential PLA2R1 staining proportions are shown in Fig. 4D. Kaplan Meier plots allow for the visualization of worse PFI (Fig. 4E) and OS (**Figure S4B)** in patients with the upper tertile of PLA2R1 staining percentage.

Table 1
Univariable and multivariable Cox analyses of IHC data

Variable		Univariable		Multivariable	
		HR (95% CI)	p-value	HR (95% CI)	p-value
Progression-Free Interval					
PLA2R1% positivity	Upper tertile vs. lower tertiles	5.2 (1.5–17.5)	0.0078	7.8 (1.8–32.7)	0.0052
Extent of resection	STR vs. GTR	3.1 (0.8–11.5)	0.0894	5.6 (1.3–25.0)	0.0228
Adjuvant radiotherapy	No vs. Yes	1.7 (0.6–5.1)	0.3185	3.2 (0.8–12.6)	0.0921
Overall Survival					
PLA2R1% positivity	Upper tertile vs. lower tertiles	6.7 (1.7–27.0)	0.0076	11.5 (1.6–80.7)	0.0144
Extent of resection	STR vs. GTR	0.9 (0.2–3.7)	0.8999	0.5 (0.1–2.4)	0.3934
Adjuvant radiotherapy	No vs. Yes	2.6 (0.7–9.7)	0.1590	0.4 (0.1–2.9)	0.3933

Functional validation shows essentiality of cell surface targets in chordoma cell lines

To evaluate the functional role of these two cell surface proteins in chordoma, we used siRNA knockdown to assess their essentiality in chordoma cell lines. The siRNA knockdowns were performed on U-CH17M and U-CH17S and an additional independent chordoma cell line UM-Chor1. The siRNA transfections were performed at 5 nM with 3 different siRNAs for each target, and a pool of all three siRNAs mixed at 1 nM each for a total concentration of 3 nM. After 24 and 48 hours of siRNA transfections, Western blot analysis was performed to assess target protein downregulation in chordoma cell lines. These results revealed reduction of PLA2R1 expression in treated cells compared to control cells (Mock, non-treated and scramble) in all chordoma cell lines after 24 and 48 hours **(**Fig. 5A**)**. The siRNA knockdowns for SLC6A12 did not show reduction in SLC6A12 expression compared to controls in U-CH17M and U-CH17S chordoma cell lines (**Figure S4C-D)**. Consequently, SLC6A12 was not included for functional evaluation. After confirming the knockdown of PLA2R1, colony formation assays were performed. Colony formation of cells transfected with siRNA targeting PLA2R1 drastically decreased colony formation ability compared to controls, suggesting a role for PLA2R1 in chordoma cell survival and proliferation.

Discussion

Chordoma is rare bone cancer of the skull base and spine originating from notochordal remnants (1, 27, 28). Despite comprehensive surgical resection and adjuvant radiation therapy, local recurrence and metastasis occur in chordoma patients which leads to devastating neurological morbidities and mortality (29). Currently there are no FDA approved drugs for treating chordomas (30–32), and lack of therapeutic interventions has led to a growing interest in understanding the proteome of chordomas to find potential therapeutic targets in order to prevent or treat disease progression and improve clinical outcomes.

Cell surface proteins are attractive therapeutic targets yet are challenging to profile with typical proteomic workflows. Several cell surface protein enrichment techniques such as the cationic colloidal silica-bead method (11), cell surface capture (CSC) (33) and *N*-glycopeptide capture (34, 35) have been established. These technologies have benefits and shortcomings, depending on the type of biological sample and starting material (7). In this project, we have used a cationic colloidal silica-bead method coupled with organelle fractionation to perform deep proteomic analyses of chordoma cell lines. These comprehensive data were mined with the goal of discovering novel chordoma cell-surface markers. We utilized subtractive proteomics to filter plasma membrane proteins against all the other organelle fractions. This proteomic approach is an efficient way to identify components/proteins of one cellular organelle from other cofractionating organelles or fractions (17). To further increase our confidence in the surface localization of our candidates, we leveraged the cell-surface protein bioinformatics tool SurfaceGenie (18). This resulted in 120 chordoma associated cell surface proteins for further evaluation.

In order select novel chordoma-enriched targets, we utilized public proteomics data of 142 cancer cell lines (19–22). This comparison was aimed to detect cell surface proteins highly enriched in chordoma with limited detection in other cancer cell lines. As there are no cell line models mimicking the normal state of the notochord, it is difficult to experimentally characterize cancer associated proteins compared to normal state (Notochord). Instead, several publicly available normal tissue datasets were used to prioritize chordoma enriched cell-surface proteins. Specifically, we used antibody staining from the Human Protein Atlas (23), two comprehensive MS-based proteomics datasets of normal human tissues (24, 25) and normal tissue transcriptional profiles from the GTEx portal (26) to evaluate the expression of chordoma cell surface proteins at the transcript and protein level in normal tissues. The goal was to prioritize chordoma specific cell surface proteins, with minimal expression in normal tissues. This systematic evaluation is important for developing targeted therapies, in order to minimize potential toxicities in normal tissue where expression of these targets may be at high levels (36–38). This resulted in prioritization of PLA2R1 and SLC6A12, as putative targets. The expression of these proteins was also confirmed in our chordoma patient cohort using IHC staining. The IHC analysis showed PLA2R1 and SLC6A12 expression to be localised to cell membranes and present within majority of chordoma patient tissue samples in various degrees.

Brachyury is a well-known biomarker for chordoma (39, 40) that is present in all samples and utilized for neuropathological diagnosis. Unfortunately, brachyury has no clinical utility for patient prognostication and there are limited prognostic indicators that exist for chordoma. In this study we found chordoma patients with elevated PLA2R1 expression had a significantly worse prognosis including overall survival

and disease-free interval. Our findings suggest PLA2R1 may have prognostic value for chordoma and could potentially be utilized clinically to identify high-risk patients that may benefit from more aggressive treatment. Biochemically, PLA2R1 is a type I transmembrane receptor, belonging to the mannose receptor family that binds several secreted phospholipases A2 (sPLA2s), collagen and carbohydrates (41, 42). The detailed role of PLA2R1 in cancer is yet to be determined, but several studies have shown that PLA2R1 has a tumor suppressive role in several other cancers (41, 43) and shown aberrant expression in prostate cancer (44). To assess the role of PLA2R1 in chordoma, we downregulated protein expression via PLA2R1 specific siRNAs. We found a significant reduction in cell growth and proliferation in all three chordoma cell lines, suggesting that PLA2R1 plays an essential role in chordoma cell growth. The related signaling pathways and underlying mechanism of PLA2R1 in chordoma need to be explored in the future.

In addition, IHC analysis demonstrated expression of SLC6A12 in most patient samples and it may be useful to pursue as potential chordoma therapeutic target. Notable, SLC6A12 expression was higher in skull base chordoma compared to the spinal chordomas, suggesting that future therapeutics strategies towards this marker may show preferential benefit for chordomas originating from the skull base, as skull base chordoma have variable clinical progression, with frequent recurrence largely due to incomplete tumor resection (45). SLC6A12 is a member of the solute carrier family involved in uptake of GABA and betaine by sodium- and chloride-dependent mechanism (46). Its precise role in cellular pathogenesis, including in cancer, are still being investigated. Specifically, it has been shown that inhibition of SLC6A12 effects *in vivo* tumor growth and proliferation in colorectal cancer by disrupting the betaine homeostasis (47). Accordingly, SLC6A12 may be an interesting protein to explore using existing small molecule inhibitors (48, 49) in future studies.

Conclusion

In conclusion, we investigated the proteome of four chordoma cell lines, revealing several novel cell surface protein candidates. The protein expression of PLA2R1 and SLC6A12 was confirmed through IHC staining of an in-house cohort of chordoma patient samples. Our results demonstrated that higher PLA2R1 expression is associated with poor prognosis and SLC6A12 expression was higher in the skull base chordomas compared to spinal chordomas. The siRNA-mediated knockdown of PLA2R1 decreased cell growth and proliferation, therefore suggesting PLA2R1 has a therapeutic potential in chordomas, however, mechanistic and *in vivo* studies are needed in the future to further elucidate the role of these proteins in chordoma.

Abbreviations

WGS
Whole genome sequence
WES
Whole exome sequence
PLA2R1

Secretory phospholipase A2 receptor

SLC6A12

Sodium- and chloride-dependent betaine transporter

BGT1

Betaine-GABA transporter

PSG

Penicillin-streptomycin-glutamine

PAA

Polyacrylic acid

TFE

2,2,2,-Trifluoroethanol

DTT

Dithiothreitol

iBAQ

Intensity-based absolute quantification

LFQ

label-free quantitation

PVDF

polyvinylidene fluoride membrane

TBST

Tris-buffered saline Tween-20

FFPE

formalin-fixed paraffin embedded

IHC

Immunohistochemistry

PCA

Principal component analysis

GS

Genie score

SPC

Surface prediction consensus score

HPA

Human protein atlas

PFI

Progression free survival

OS

overall survival

CSC

cell surface capture

sPLA2s

secreted phospholipases A2

Declarations

Ethics approval and consent to participate

This study was approved by the Research Ethics Board of University Health Network, Toronto. Chordoma patients FFPE slides and clinical follow up data were obtained from the University Health Network Biobank (REB# - 18-5820).

Consent for publication

This manuscript has been read and approved by all the authors to publish and is not submitted or under consideration for publication elsewhere.

Availability of data and materials

All mass spectrometry raw data has been deposited to the Mass Spectrometry Interactive Virtual Environment (MassIVE) with the following accession MSV000089171 at ftp://MSV000089171@massive.ucsd.edu.

Competing interests

The funders had no role in the design of the study; the collection, analysis, and interpretation of the data; the writing of the manuscript; and the decision to submit the manuscript for publication. The authors have no conflicts of interest to disclose.

Funding

This work was supported by a CIHR Project grant (PJT162384) to T.K. and a Canadian Cancer Society Operating Grant (706135) to G.Z., TK is supported through the Canadian Research Chair program. M.G. was supported by an OGS Graduate student fellowship, a Kristi Piia CALLUM Memorial Fellowship in Ovarian Cancer Research and a MBP Excellence OSOTF award. M.W. was supported by a Princess Margaret Postdoctoral Fellowship. J.Z. is supported by a Canadian Institute of Health Research Canada Graduate Scholarship Doctoral Award. This research was funded in part by the Ontario Ministry of Health and Long-Term Care.

Authors contributions

The corresponding authors had full access to all the data in the study and take responsibility for the integrity of the data and the accuracy of the data analysis. S.K., J.Z., G.Z., and T.K. conceived of the study idea. S.K., J.Z., V.I., O.S., M.G., and A.G., performed experiments and data analysis. S.K., J.Z., G.Z., and T.K wrote the manuscript with input from all other authors. T.K., and G.Z supervised the study. All authors interpreted the data, reviewed the manuscript and approved the final version.

Acknowledgements

We would like to thank the Chordoma Foundation for generously providing the cell line models used in this study.

References

1. McMaster ML, Goldstein AM, Bromley CM, Ishibe N, Parry DM. Chordoma: incidence and survival patterns in the United States, 1973–1995. Cancer Causes Control. 2001;12(1):1–11.
2. Zou MX, Huang W, Wang XB, Li J, Lv GH, Deng YW. Prognostic factors in spinal chordoma: A systematic review. Clin Neurol Neurosurg. 2015;139:110–8.
3. Zuccato JA, Patil V, Mansouri S, Liu JC, Nassiri F, Mamatjan Y, et al. DNA Methylation based prognostic subtypes of chordoma tumors in tissue and plasma. Neuro Oncol. 2021.
4. Tarpey PS, Behjati S, Young MD, Martincorena I, Alexandrov LB, Farndon SJ, et al. The driver landscape of sporadic chordoma. Nat Commun. 2017;8(1):890.
5. Sa JK, Lee IH, Hong SD, Kong DS, Nam DH. Genomic and transcriptomic characterization of skull base chordoma. Oncotarget. 2017;8(1):1321–8.
6. Bell D, Raza SM, Bell AH, Fuller GN, DeMonte F. Whole-transcriptome analysis of chordoma of the skull base. Virchows Arch. 2016;469(4):439–49.
7. Kuhlmann L, Cummins E, Samudio I, Kislinger T. Cell-surface proteomics for the identification of novel therapeutic targets in cancer. Expert Rev Proteomics. 2018;15(3):259–75.
8. Boisvert FM, Lam YW, Lamont D, Lamond AI. A quantitative proteomics analysis of subcellular proteome localization and changes induced by DNA damage. Mol Cell Proteomics. 2010;9(3):457–70.
9. Bausch-Fluck D, Goldmann U, Müller S, van Oostrum M, Müller M, Schubert OT, et al. The in silico human surfaceome. Proc Natl Acad Sci U S A. 2018;115(46):E10988-e97.
10. Yin H, Flynn AD. Drugging Membrane Protein Interactions. Annu Rev Biomed Eng. 2016;18:51–76.
11. Chaney LK, Jacobson BS. Coating cells with colloidal silica for high yield isolation of plasma membrane sheets and identification of transmembrane proteins. J Biol Chem. 1983;258(16):10062–72.
12. Kim Y, Elschenbroich S, Sharma P, Sepiashvili L, Gramolini AO, Kislinger T. Use of colloidal silica-beads for the isolation of cell-surface proteins for mass spectrometry-based proteomics. Methods Mol Biol. 2011;748:227–41.
13. Kislinger T, Rahman K, Radulovic D, Cox B, Rossant J, Emili A. PRISM, a generic large scale proteomic investigation strategy for mammals. Mol Cell Proteomics. 2003;2(2):96–106.
14. Kislinger T, Cox B, Kannan A, Chung C, Hu P, Ignatchenko A, et al. Global survey of organ and organelle protein expression in mouse: combined proteomic and transcriptomic profiling. Cell. 2006;125(1):173–86.

15. Kurganovs N, Wang H, Huang X, Ignatchenko V, Macklin A, Khan S, et al. A proteomic investigation of isogenic radiation resistant prostate cancer cell lines. Proteomics Clin Appl. 2021;15(5):e2100037.
16. Nassiri F, Liu J, Patil V, Mamatjan Y, Wang JZ, Hugh-White R, et al. A clinically applicable integrative molecular classification of meningiomas. Nature. 2021;597(7874):119–25.
17. Schirmer EC, Florens L, Guan T, Yates JR, 3rd, Gerace L. Nuclear membrane proteins with potential disease links found by subtractive proteomics. Science. 2003;301(5638):1380–2.
18. Waas M, Snarrenberg ST, Littrell J, Jones Lipinski RA, Hansen PA, Corbett JA, et al. SurfaceGenie: a web-based application for prioritizing cell-type-specific marker candidates. Bioinformatics. 2020;36(11):3447–56.
19. Gholami AM, Hahne H, Wu Z, Auer FJ, Meng C, Wilhelm M, et al. Global proteome analysis of the NCI-60 cell line panel. Cell Rep. 2013;4(3):609–20.
20. Lawrence RT, Perez EM, Hernández D, Miller CP, Haas KM, Irie HY, et al. The Proteomic Landscape of Triple-Negative Breast Cancer. Cell Rep. 2015;11(6):990.
21. Coscia F, Watters KM, Curtis M, Eckert MA, Chiang CY, Tyanova S, et al. Integrative proteomic profiling of ovarian cancer cell lines reveals precursor cell associated proteins and functional status. Nat Commun. 2016;7:12645.
22. Wang J, Mouradov D, Wang X, Jorissen RN, Chambers MC, Zimmerman LJ, et al. Colorectal Cancer Cell Line Proteomes Are Representative of Primary Tumors and Predict Drug Sensitivity. Gastroenterology. 2017;153(4):1082–95.
23. Uhlén M, Fagerberg L, Hallström BM, Lindskog C, Oksvold P, Mardinoglu A, et al. Proteomics. Tissue-based map of the human proteome. Science. 2015;347(6220):1260419.
24. Jiang L, Wang M, Lin S, Jian R, Li X, Chan J, et al. A Quantitative Proteome Map of the Human Body. Cell. 2020;183(1):269 – 83.e19.
25. Wang D, Eraslan B, Wieland T, Hallström B, Hopf T, Zolg DP, et al. A deep proteome and transcriptome abundance atlas of 29 healthy human tissues. Mol Syst Biol. 2019;15(2):e8503.
26. The Genotype-Tissue Expression (GTEx) project. Nat Genet. 2013;45(6):580–5.
27. Bai J, Shi J, Li C, Wang S, Zhang T, Hua X, et al. Whole genome sequencing of skull-base chordoma reveals genomic alterations associated with recurrence and chordoma-specific survival. Nat Commun. 2021;12(1):757.
28. Salisbury JR, Deverell MH, Cookson MJ, Whimster WF. Three-dimensional reconstruction of human embryonic notochords: clue to the pathogenesis of chordoma. J Pathol. 1993;171(1):59–62.
29. Yang Y, Niu X, Li Y, Liu W, Xu H. Recurrence and survival factors analysis of 171 cases of sacral chordoma in a single institute. Eur Spine J. 2017;26(7):1910–6.
30. Thanindratarn P, Dean DC, Feng W, Wei R, Nelson SD, Hornicek FJ, et al. Cyclin-dependent kinase 12 (CDK12) in chordoma: prognostic and therapeutic value. Eur Spine J. 2020;29(12):3214–28.
31. Thanindratarn P, Dean DC, Nelson SD, Hornicek FJ, Duan Z. T-LAK cell-originated protein kinase (TOPK) is a Novel Prognostic and Therapeutic Target in Chordoma. Cell Prolif. 2020;53(10):e12901.

32. Stacchiotti S, Sommer J. Building a global consensus approach to chordoma: a position paper from the medical and patient community. Lancet Oncol. 2015;16(2):e71-83.
33. Wollscheid B, Bausch-Fluck D, Henderson C, O'Brien R, Bibel M, Schiess R, et al. Mass-spectrometric identification and relative quantification of N-linked cell surface glycoproteins. Nat Biotechnol. 2009;27(4):378–86.
34. Zhang H, Li XJ, Martin DB, Aebersold R. Identification and quantification of N-linked glycoproteins using hydrazide chemistry, stable isotope labeling and mass spectrometry. Nat Biotechnol. 2003;21(6):660–6.
35. Cogger KF, Sinha A, Sarangi F, McGaugh EC, Saunders D, Dorrell C, et al. Glycoprotein 2 is a specific cell surface marker of human pancreatic progenitors. Nat Commun. 2017;8(1):331.
36. Stepan LP, Trueblood ES, Hale K, Babcook J, Borges L, Sutherland CL. Expression of Trop2 cell surface glycoprotein in normal and tumor tissues: potential implications as a cancer therapeutic target. J Histochem Cytochem. 2011;59(7):701–10.
37. Zhao Z, Ukidve A, Kim J, Mitragotri S. Targeting Strategies for Tissue-Specific Drug Delivery. Cell. 2020;181(1):151–67.
38. Kumar V, Sanseau P, Simola DF, Hurle MR, Agarwal P. Systematic Analysis of Drug Targets Confirms Expression in Disease-Relevant Tissues. Sci Rep. 2016;6:36205.
39. Vujovic S, Henderson S, Presneau N, Odell E, Jacques TS, Tirabosco R, et al. Brachyury, a crucial regulator of notochordal development, is a novel biomarker for chordomas. J Pathol. 2006;209(2):157–65.
40. Oakley GJ, Fuhrer K, Seethala RR. Brachyury, SOX-9, and podoplanin, new markers in the skull base chordoma vs chondrosarcoma differential: a tissue microarray-based comparative analysis. Mod Pathol. 2008;21(12):1461–9.
41. Vindrieux D, Augert A, Girard CA, Gitenay D, Lallet-Daher H, Wiel C, et al. PLA2R1 mediates tumor suppression by activating JAK2. Cancer Res. 2013;73(20):6334–45.
42. Jaber S, Goehrig D, Bertolino P, Massemin A, Bihl F, Chabry J, et al. Generation of a conditional transgenic mouse model expressing human Phospholipase A2 Receptor 1. Sci Rep. 2020;10(1):8190.
43. Augert A, Vindrieux D, Girard CA, Le Calvé B, Gras B, Ferrand M, et al. PLA2R1 kills cancer cells by inducing mitochondrial stress. Free Radic Biol Med. 2013;65:969–77.
44. Friedemann M, Nacke B, Hagelgans A, Jandeck C, Bechmann N, Ullrich M, et al. Diverse effects of phospholipase A2 receptor expression on LNCaP and PC-3 prostate cancer cell growth in vitro and in vivo. Oncotarget. 2018;9(89):35983–96.
45. Jones PS, Aghi MK, Muzikansky A, Shih HA, Barker FG, 2nd, Curry WT, Jr. Outcomes and patterns of care in adult skull base chordomas from the Surveillance, Epidemiology, and End Results (SEER) database. J Clin Neurosci. 2014;21(9):1490–6.
46. Kempson SA, Zhou Y, Danbolt NC. The betaine/GABA transporter and betaine: roles in brain, kidney, and liver. Front Physiol. 2014;5:159.

47. Jang YS, Jo YK, Sim JJ, Ji E, Jeong KY, Kim HM. Lactate calcium salt affects the viability of colorectal cancer cells via betaine homeostasis. Life Sci. 2016;147:71–6.
48. Dalby NO, Thomsen C, Fink-Jensen A, Lundbeck J, Søkilde B, Man CM, et al. Anticonvulsant properties of two GABA uptake inhibitors NNC 05-2045 and NNC 05-2090, not acting preferentially on GAT-1. Epilepsy Res. 1997;28(1):51–61.
49. Borden LA, Dhar TG, Smith KE, Branchek TA, Gluchowski C, Weinshank RL. Cloning of the human homologue of the GABA transporter GAT-3 and identification of a novel inhibitor with selectivity for this site. Recept Channels. 1994;2(3):207–13.

Figures

Fig. 1

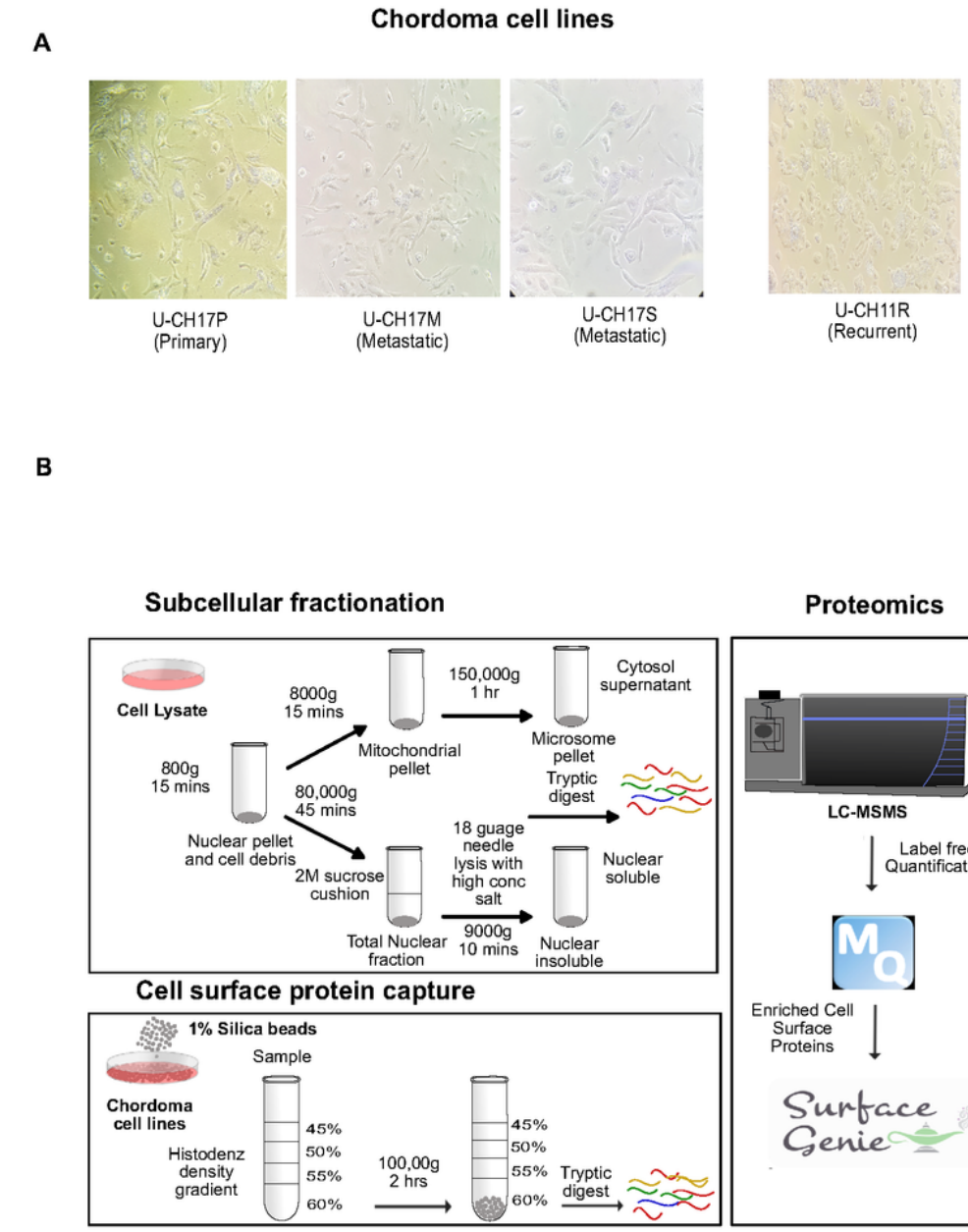

Figure 1

Schematics of silica-bead based surface protein capture and organelle fractionation: A) Chordoma cell lines, CH17P (Primary), U-CH17M (Metastatic), UCH17S (Metastatic) (derived from same patient, male, age 34, with sacral chordoma) and U-CH11R (Recurrent) (derived from male patient, age 75, with sacral chordoma) used for proteomics analysis. B) Schematic representation of cell-surface capture, using the

colloidal silica-bead method and organelle fractionation using ultracentrifugation combined with MS-based proteomics.

Fig. 2

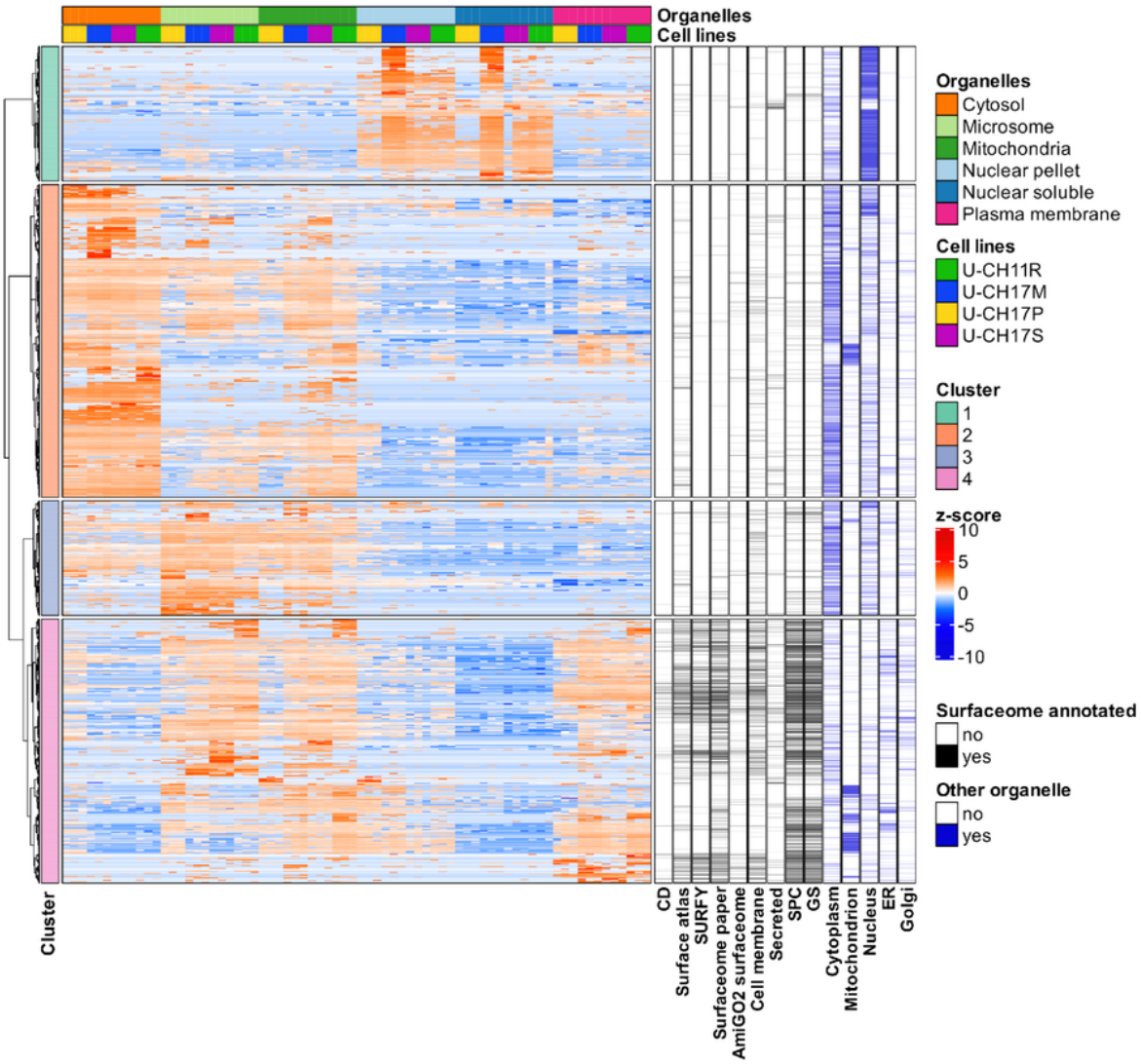

Figure 2

Analysis of sub-cellular proteomes. Heatmap showing four distinct protein clusters using unsupervised hierarchal clustering based on protein abundance (z-score) of all proteins detected. The annotations on the righthand side (black) indicate surface localization annotation based on several public databases and organelle localization annotation from Uniprot (blue). Other covariates (cell line, organelle type and clusters) are shown in the annotation bars on the right. The annotation on the top indicates the cell line and organelle type.

Fig. 3

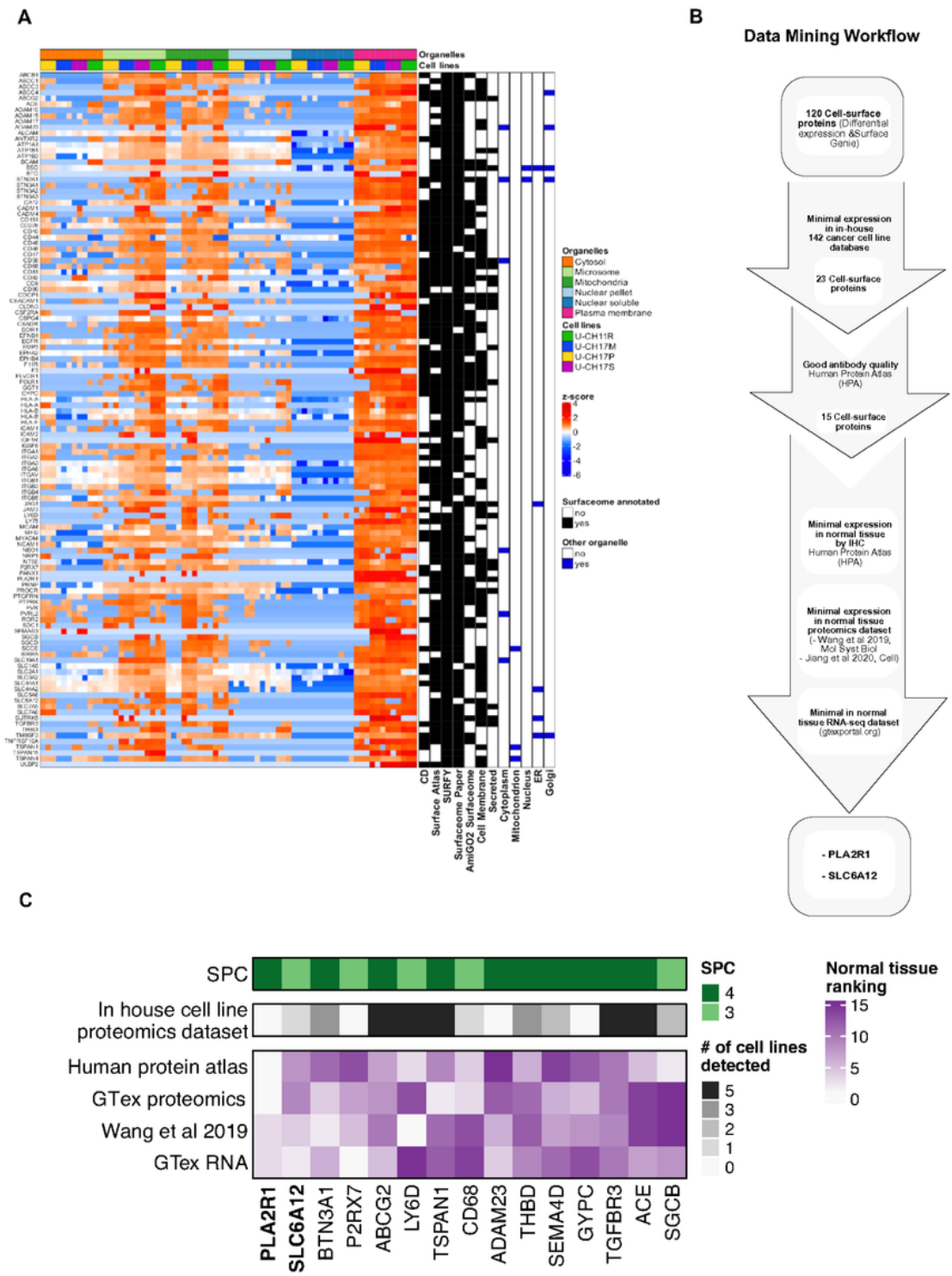

Figure 3

Mining of surface proteins. A) Heatmap of 120 enriched cell-surface proteins. B) Cell surface protein mining strategy, where the 120 proteins were first filtered for proteins with limited expression in other cancers and antibody availability. The remaining 15 proteins were then ranked based on normal tissue expression in by IHC (23), median protein expression (24, 25), and median RNA expression in normal tissue datasets (26). The ranks across all four normal tissue datasets were summed and the two highest

ranking proteins, PLA2R1 and SLC6A12, were selected for further evaluation. C) Heatmap showing the ranking of selected cell-surface proteins in normal tissue datasets, HPA (23), two proteomics datasets (24, 25) and GTex RNA-seq data (26). The SPC score and number of cell lines these proteins were detected in public proteomics datasets are shown on top.

Figure 4

Selection and validation of two chordoma surface proteins. A) Testing the expression of PLA2R1 and SLC6A12 target proteins in chordoma cell lines (U-CH17M, U-CH17S and U-CH11R), chordoma tissues and commercially available normal tissue lysates by Western blots**.** B) Representative IHC images showing a higher proportion of SLC6A12 in skull-base than spinal chordomas. C) Boxplots showing higher SLC6A12 positive cellularity in skull base versus spinal chordomas D), The variability of PLA2R1 expression among tumor samples grouped into an upper tertile and lower two-thirds of expression for visualization. E) Kaplan Meier plot showing poorer PFI in the top third of patients according to percent of cells positive for PLA2R by IHC.

Fig. 5

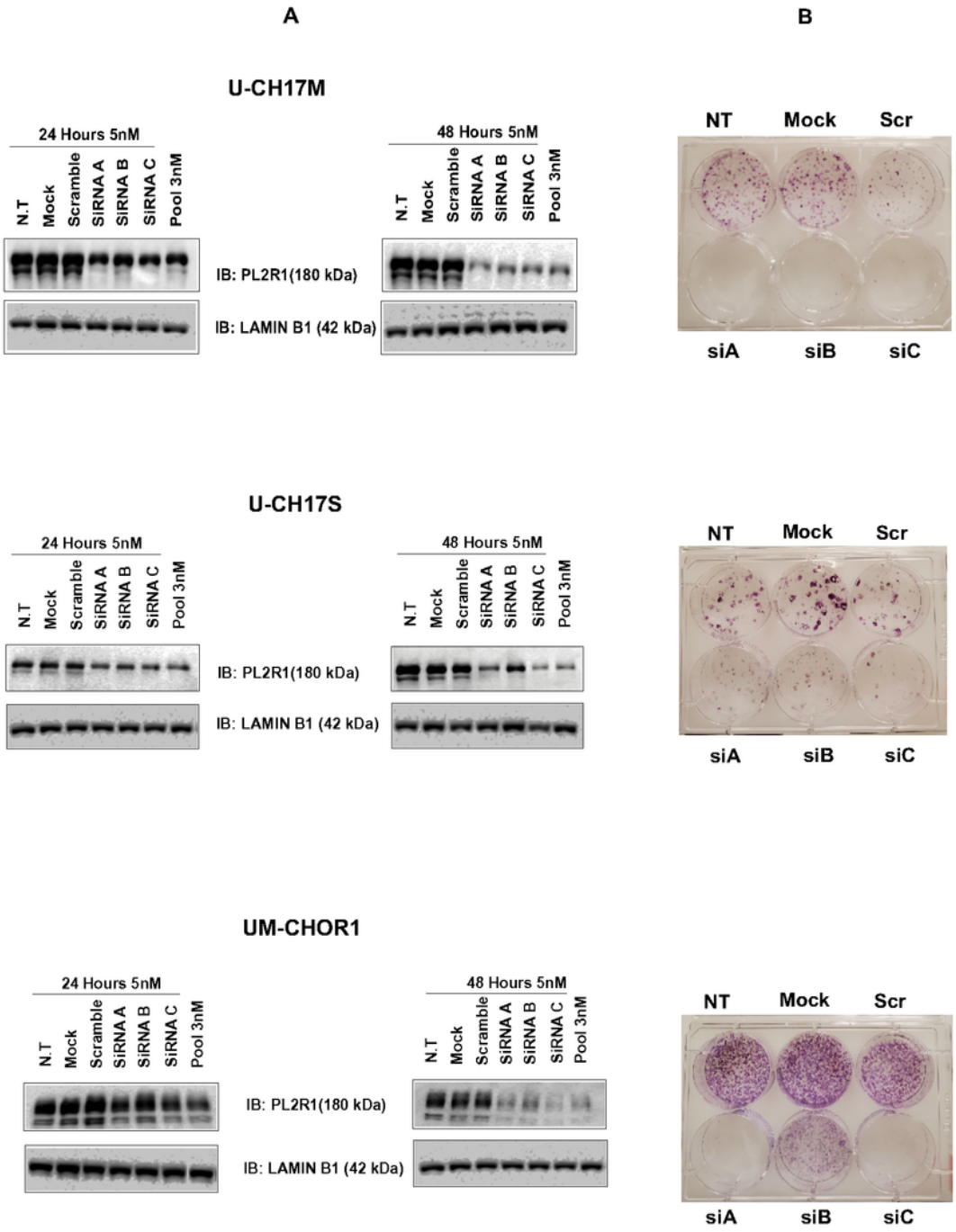

Figure 5

A) Effect of siRNA knockdown on cell growth and survival. A) Expression of PLA2R1 in U-CH17M, U-CH17S and UM-Chor1 following siRNA-mediated knockdown (24 and 48 hours). B) Digital image of colony formation assay after siRNA knockdown.

Supplementary Files

This is a list of supplementary files associated with this preprint. Click to download.

- Supplementaryfigures.pdf
- TableS1.xlsx